Prestressed CFRP Strips for Concrete Bridge Girder Retrofitting: Application and Static Loading Test

Julien Michels, Ph.D.[1]; Michał Staśkiewicz[2]; Christoph Czaderski, Ph.D.[3]; Renata Kotynia, Ph.D.[4]; Yunus Emre Harmanci[5]; and Masoud Motavalli, Ph.D., M.ASCE [6]

Abstract: This paper presents an investigation on the practicability and structural efficiency of prestressed carbon-fiber–reinforced polymer (CFRP) strips with a gradient anchorage in the framework of a bridge-strengthening application in Poland. The nonmechanical anchorage system avoids the installation of metallic bolts and plates, with the exception of a temporary support frame. Two 18.4-m-long large-scale prestressed concrete girders were produced following the drawings of the existing bridge construction. One girder served as a reference, and the second one was strengthened with two prestressed CFRP strips. In this case, the initial negative cambering was leveled out by a layer of dry shotcrete. CFRP strips with a prestrain of 0.58% were applied for flexural upgrading. Both girders with a total length of 18.4 m were finally statically loaded up to failure to assess the strengthening efficiency in flexure of the retrofitting technique used. Tensile failure of the CFRP strips was reached, indicating an optimal use of the composite reinforcement. The strengthened girder exhibited a ductile behavior up to strip rupture with a distinct steel yielding and a subsequent pronounced increase of the load-carrying capacity. For service load considerations, an enhancement of the cracking load of approximately 16% was noticed. In terms of ultimate load, a significant improvement of approximately 25% compared to the reference girder was reached. Although some practical problems need optimization, the presented results are very promising and make this strengthening system an alternative for future retrofitting applications in bridge engineering. **DOI: 10.1061/(ASCE)BE.1943-5592.0000835.**

Author keywords: Prestressed concrete bridge girder; Flexural and shear strengthening; Prestressed CFRP strips; Dry shotcrete; Static testing.

Background

The application of carbon-fiber–reinforced polymer (CFRP) strips in structural strengthening is well accepted today (Meier 1995; Bakis et al. 2002). Their use in the civil engineering domain has drastically increased over the last three decades, and several available design codes and recommendations (see fib 2001; ACI 2008; SIA 2004; DAfStb 2012) attest to their popularity. Applications with initially unstressed CFRP strips as an externally bonded reinforcement (EBR) or near-surface mounted (NSM) technique in bridge engineering can be found (Blaschko and Zehetmaier 2008; Petrou et al. 2008; Bae and Belarbi 2013; Cerullo et al. 2013; Kasan et al. 2014). For example, an onsite failure test of a CFRP-strengthened railway concrete bridge is presented by Puurula et al. (2014). However, strengthening with prestressed CFRP laminates has surprisingly not known a similar success despite the undeniable advantages, such as reduction of crack widths, reduction of deflections, as well as increased cracking, yielding, and ultimate load (El-Hacha et al. 2001; Wight et al. 2001; Pellegrino and Modena 2009; Michels et al. 2013). Moreover, the strip prestressing usually involves a much more efficient use of the composite's excellent mechanical properties, mainly the high tensile strength. Whereas an initially unstressed strip failure generally occurs by strip debonding at strain levels below 1.0%, an initial prestrain can shift the maximum strains close to tensile failure (Meier and Stöcklin 2005; Suter and Jungo 2001; Kotynia et al. 2011). A key factor in prestressing is the anchorage system. Nowadays, most available solutions (commercially available and at the laboratory level) are so-called *mechanical* systems, which utilize mechanical plates and bolts at the strip ends to avoid debonding (Berset et al. 2002; El-Hacha et al. 2003; Pellegrino and Modena 2009; Xue et al. 2008). One example of the few applications of prestressed CFRP sheets in a bridge retrofitting project is given in Kim et al. (2008).

The *gradient anchorage* applies a gradual prestress force release with intermediate accelerated adhesive curing at both strip ends until no pressure remains in the hydraulic system. It is based on the ability of the epoxy resin to develop strength and stiffness faster under high temperatures (Czaderski et al. 2012). Early research was

[1]Project Leader, Empa, Structural Engineering Research Laboratory, Swiss Federal Laboratories for Materials Science and Technology, Überlandstrasse 129, Dübendorf CH-8600, Switzerland (corresponding author). E-mail: julien.michels@empa.ch

[2]Ph.D. Candidate, Dept. of Concrete Structures, Łódź Univ. of Technology, 90-924 Łódź, Poland. E-mail: michal.staskiewicz@p.lodz.pl

[3]Senior Scientist, Empa, Structural Engineering Research Laboratory, Swiss Federal Laboratories for Materials Science and Technology, Überlandstrasse 129, Dübendorf CH-8600, Switzerland. E-mail: christoph.czaderski@empa.ch

[4]Associate Professor, Dept. of Concrete Structures, Łódź Univ. of Technology, 90-924 Łódź, Poland. E-mail: renata.kotynia@p.lodz.pl

[5]Research Assistant, ETHZ, Swiss Federal Institute of Technology Zurich, Institute of Structural Engineering, Stefano-Franscini-Platz 5, CH-8093 Zürich, Switzerland; Empa, Swiss Federal Laboratories for Materials Science and Technology, Structural Engineering Research Laboratory, Überlandstrasse 129, CH-8600 Dübendorf, Switzerland. E-mail: harmanci@ibk.baug.ethz.ch

[6]Professor, Laboratory Head, Empa, Structural Engineering Research Laboratory, Swiss Federal Laboratories for Materials Science and Technology, Überlandstrasse 129, Dübendorf CH-8600, Switzerland. E-mail: masoud.motavalli@empa.ch

Note. This manuscript was submitted on February 6, 2015; approved on July 16, 2015; published online on January 20, 2016. Discussion period open until June 20, 2016; separate discussions must be submitted for individual papers. This paper is part of the ***Journal of Bridge Engineering***, © ASCE, ISSN 1084-0702.

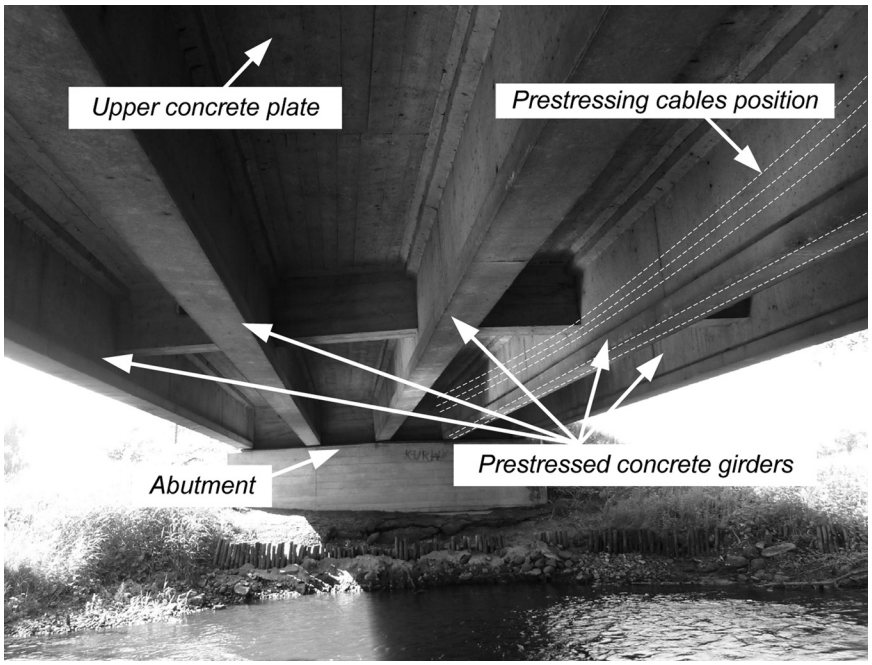

Fig. 1. Bottom view of the road bridge in Poland before retrofitting (image by Julien Michels)

documented by Meier et al. (2001), Kotynia et al. (2011), and Michels et al. (2013).

The final step was the flexural upgrading of a road bridge in Szczercowska Wieś, Poland (see Fig. 1). The bridge was built in the 1960s and is composed of five simply supported simple-span prestressed concrete (PC) girders and a RC deck. The girders were precast and delivered to the construction site, and the plate was cast on site. In the framework of the strengthening project in 2014, the upper deck was replaced by a thicker plate. The current cross section of the old bridge is given in Fig. 2. Each girder was prestressed with three parabolic cables and two straight cables in the bottom flange (see Fig. 3). The two principal aims of this investigation are as follows: (1) verify the practicability of the technique in such a bridge-strengthening case, and (2) assess the structural efficiency when two prestressed CFRP strips with a gradient anchorage are used for flexural upgrading of one girder. For this purpose, two girders were reproduced according to the original drawings and subsequently tested under static loading. Whereas one served as a reference, the second was strengthened with two prestressed CFRP strips with gradient anchorage prior to testing. Additionally, a shear reinforcement in compliance with the Polish PN-91/S-10042 standard (Polish Committee for Standardization 1991) was applied in the form of CFRP wraps. This paper presents the girder production, the different strengthening steps, as well as the final static tests and the related results.

Girder Fabrication

This section briefly summarizes key material characteristics and explains the different production and prestressing steps.

Materials and Girder Production

Because of the slender geometry of the girders, a self-compacting concrete (C35/45) with a maximum aggregate size ($d_{\max}$) of 16 mm was chosen for casting. The upper slabs were casted with a regular C30/37 with a maximum aggregate size of 16 mm and a *w*/*c* ratio of 0.49. Compressive strength (f_{cm}), tested on $150 \times 150 \times 150$-mm^3 cubes, and elastic modulus (E_{cm}), tested on $120 \times 120 \times 360$-mm^3 prisms, are given at 28 days and at the testing day in Table 1.

Yield strength, ultimate tensile strength, and strain at failure of the reinforcing steel bars with diameters ($\varnothing$) of 6 and 8 mm are summarized in Table 2. For the structural assessment to be as realistic as possible, the passive steel reinforcement had no ribs.

Prestressing tendons had a total cross section (A_p) of 345 mm^2. The average yield limit ($R_{p,0.1}$) at 0.1% strain was approximately 1,660 MPa, and the average ultimate strength (R_m) was approximately 1,810 MPa according to the testing certificate provided by the distributor. The average elastic modulus (E_{nom}) was 201.3 GPa, and average strain at failure (A_g) was 3.76%.

After casting, the second fabrication step comprises the prestressing of three parabolic and two straight steel tendons (see Fig. 4). Each tendon was prestressed to an initial prestressing force ($F_{fp,0}$) of approximately 363 kN. Initial negative cambers at a midspan of approximately 33 mm were measured for Girders 1 and 2. In this case, calculated compression stress on the bottom fiber was 28 MPa, slightly below 50% of the compressive strength. For the weeks following the prestressing application, creep behavior was monitored. Fig. 5 presents the evolution of the negative deflection at the girder midspan. Last, a part of the new upper concrete deck with a width of 125 cm and a thickness of 21 cm was casted. The complete cross section is shown in Fig. 6.

For flexural strengthening, a commercially available two-component epoxy resin was used. The CFRP strips had a width (b_f) of 100 mm and a thickness (t_f) of 1.2 mm. According to the distributor, the strips have a nominal elastic modulus (E_f) of 165 GPa, which was used later for deriving the total prestressing force from the measured prestrain. Tensile tests on small strip specimens were performed according to DIN-EN-ISO-527-5 (DIN 1997) and revealed a undirectional tensile strength ($f_{f,u}$) of 2,795 ($\pm$115) MPa at an average failure strain of 1.6%. CFRP wraps with an elastic modulus (E_f) above 240 GPa and a strain at failure ($\varepsilon_{f,u}$) of 1.7% were installed as shear reinforcement.

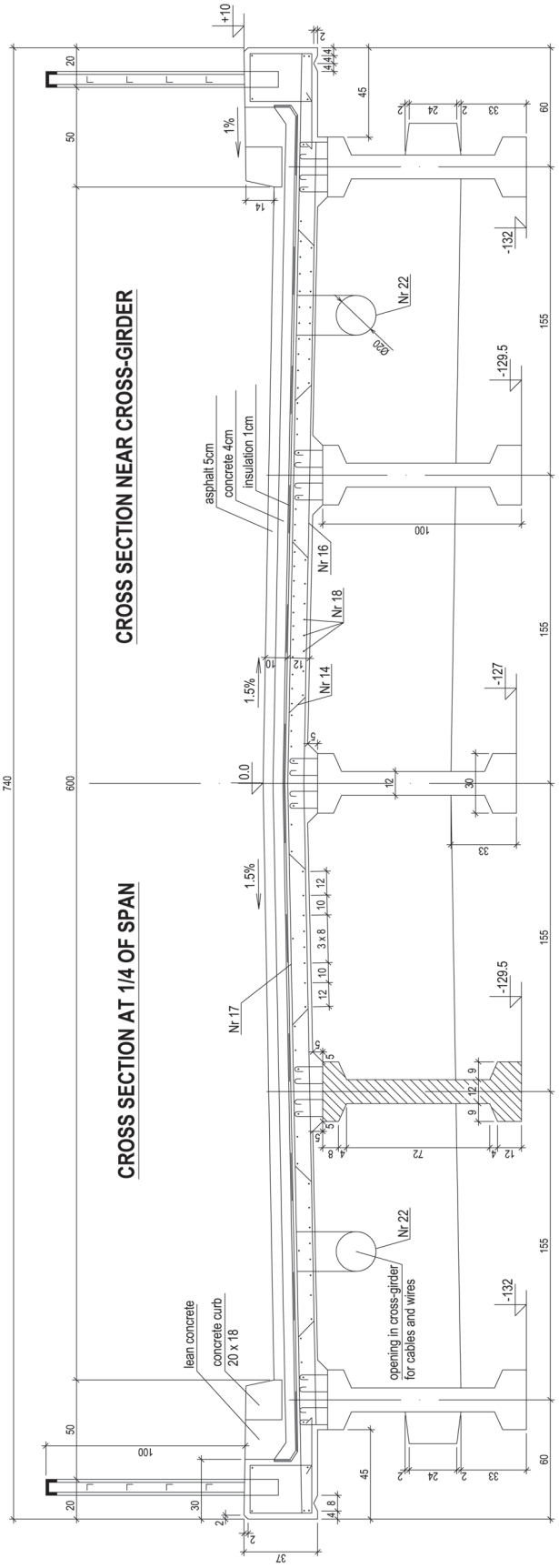

Fig. 2. Bridge cross section before retrofitting (dimensions in centimeters)

These and several other characteristics can be taken from the referenced data sheet.

Surface Leveling

The surface-leveling procedure was chosen according to a preceding experimental investigation on the bond behavior of CFRP strips with various cementitious substrates (Michels et al. 2014). Prior to the shotcrete application, the bottom surface of the girder was roughened by high-pressure waterjetting (see Fig. 7). Subsequently, dry shotcrete with a maximum aggregate diameter (d_{max}) of 8 mm and a guaranteed compressive strength of 60 MPa after 28 days was applied. The application, for which the girder was covered with a plastic plane for protection against the strong rebound and dust formation, is presented in Fig. 7. On the day of the shotcrete application, which took place more than a year after the last reading of Fig. 5, the maximum camber level at midspan was approximately 60 mm.

Flexural Strengthening

Each CFRP strip was prestressed to a strain level ($\varepsilon_{fp,0}$) of 0.58%, which corresponds to a prestressing force ($F_{fp,0}$) of approximately 115 kN, calculated with the previously indicated elastic modulus of 165 GPa. Because two strips were applied, an additional 230 kN was introduced into the girder cross section. The gradient anchorage at the strip ends was realized by following a program identical to that described by Michels et al. (2013) [i.e., three consecutive force releases (ΔF) of 50, 35, and 35 kN over 300-, 200-, and 200-mm bond lengths, respectively]. In terms of prestressing technique, a *prestressing against the structure* (El-Hacha et al. 2001) was applied. Because of the slender geometry and the inner prestressing steel tendons, drilling of the girder was not allowed, and thus a temporary steel frame, responsible for the force transfer to the girder during the prestressing, was mounted by adhesive bonding. Despite an initial debonding of the first CFRP strip during the installation (which required repeating the procedure), it was eventually possible to anchor both laminates at the desired prestrain level. During the release of the second CFRP strip, a large crack appeared in the anchorage zone without, however, inducing a debonding failure. The strain level in the CFRP strip remained constant. Afterward, the crack was injected with a resin and had, as shown later in the paper, no effect on the load-carrying capacity of the girder. An adapted procedure was followed for the final bridge application. A photo of the girder bottom with two strips is shown in Fig. 8.

Shear Strengthening

The fabric had an initial width (b_f) of 30 cm, and was folded twice to obtain a final width of approximately 7.5 cm; the final wrap thickness (t_f) was approximately 1 mm. The wraps were subsequently bonded to the concrete by a wet-lay-up procedure around the total cross section to include the compression zone (Fig. 8). Prior to the application, concrete filling elements were installed to dispose of a regular cross-section geometry at the respective locations.

Cross-Section Analysis

Flexural resistance was evaluated by means of a cross-section analysis (CSA) (see Fig. 9). The complex girder geometry due to the curved inner prestress cables and the related variable cable position (d_p) along the horizontal girder axis indicates that the force equilibrium and strain compatibility have to be established on several

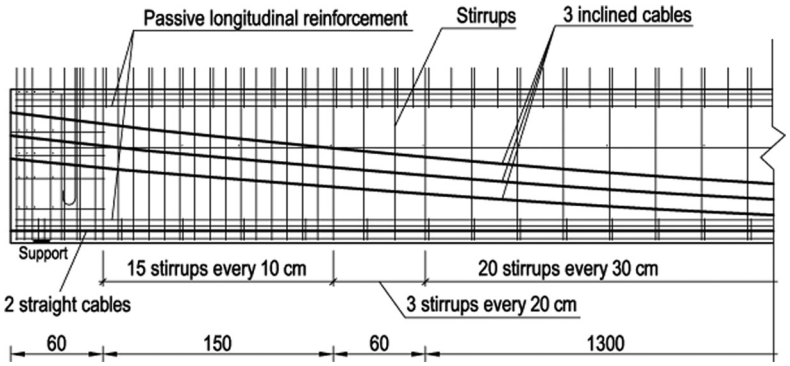

Fig. 3. Extract of flexural (passive and prestressed) and shear reinforcement over a part of the girder length (without the upper slab)

Table 1. Concrete Compressive Strength on Cube (f_{cm}) and Elastic Modulus (E_{cm}) at 28 Days and at Testing Day

	Girder 1		Plate 1		Girder 2		Plate 2	
Time	f_{cm} (MPa)	E_{cm} (GPa)	f_{cm} (MPa)	E_{cm} (GPa)	f_{cm} (MPa)	E_{cm} (GPa)	f_{cm} (MPa)	E_{cm} (GPa)
28 days	61.4	34.9	47.5	33.3	62.1	33.5	51.1	34.0
Test day	64.6	34.7	50.0	32.1	66.9	N/A	53.5	N/A

Table 2. Yield Strength, Tensile Strength, and Strain at Failure of the Passive Steel Bar Reinforcement without Ribs

∅ (mm)	R_i (MPa)	R_m (MPa)	$\varepsilon_{s,u}$ (%)
6	387	485	15.3
8	462	545	10.6

locations along the girder to derive the deflection at midspan (δ) by double integration of the curvature (χ) (Harmanci 2013). Strength values are as indicated in the "Materials and Girder Production" section. Steel reinforcements (passive and prestressed) were considered with bilinear constitutive laws, including a stiffening behavior up to failure after reaching the yield stress (see Table 2). CFRP strips were considered as perfectly linear elastic up to failure. Finally, concrete was included as linear elastic in tension until reaching tensile strength (f_{ct}); in compression, a second-degree parabola was implemented (Hognestad 1951; Park and Paulay 1975). For both the prestress steel cables and the CFRP reinforcement, prestressing was included as a prestrain at the moment of the first loading. In Fig. 9, the example of the strain state after prestressing and anchoring the CFRP strip is shown. The initial strip prestrain ($\varepsilon_{fp,0}$) increases as a result of the ongoing static loading by $\Delta\varepsilon_f$, resulting in a total strip strain (ε_f). The total concrete compressive strain corresponds to ε_c, and the total cable stress to $\varepsilon_p = \varepsilon_{p,0} + \Delta\varepsilon_p$.

Experimental Investigation: Test Setup

The test setup is presented in Figs. 10 and 11. Both girders were simply supported with a total span of 18 m. In the central third, four actuators at a distance of 1.2 m applied point loads (strip loads in the transverse direction) under displacement control at a velocity of 1 mm/min for the preloading stage, and subsequently, 3.5 mm/min for the final failure test. The loading configuration was chosen according to the Polish PN-85/S-10030 code for bridge design (Polish Committee for Standardization 1986). Several LVDTs and strain gauges were installed to measure local displacements and strains, and the locations are given in Fig. 11. Concrete compressive strain on top of the girder was measured at five locations along the girder, each time with two strain gauges over the width (SG2.1 and SG2.2 to SG6.1 and SG6.2, respectively). For Girder 2, tensile strain of both CFRP strips was recorded at the same location as the corresponding compressive strains on top, one gauge per strip (CFRP2.1, CFRP2.2–CFRP6.1, CFRP6.2). During the prestressing, two additional gauges per strip (CFRP10.1 and CFRP10.2, and CFRP20.1 and 20.2, respectively) were mounted to assess the prestrain ($\varepsilon_{fp,0}$; see Fig. 11). Finally, vertical deflections were recorded for both girders at midspan.

Results and Discussion

Force Deflection

The key results of the tests are summarized in Table 3. The force-deflection (midspan) curves (only one loading force is plotted; see Fig. 11) for both girders are given in Fig. 12, and crack patterns after test end for both Girders 1 and 2 are presented in Fig. 13. Both girders exhibited shear cracks after a certain load level, but eventually failed in flexure. Fig. 12 shows that prestressing the CFRP strips causes an increase in the cracking load (F_{cr}) from approximately 95 kN for the reference girder to 110 kN for the strengthened structure, corresponding to a relative enhancement of 16%. With a continuously increasing load, the overall structural behavior of the strengthened Girder 2 is, as expected, clearly stiffer than the reference test. For instance, an increase in bending stiffness from approximately 746 kN/m for the reference girder to 983 kN/m for the strengthened member is noticed. Because no strain gauges were used to assess the steel cable strain, the yielding load (F_y) cannot be determined exactly. Nevertheless, it becomes obvious from the loading curve that the strengthened girder exhibits a higher yielding load (Fig. 12). The reference test was conducted up to a deflection (δ_u) of 260 mm, and was stopped because of stroke limitation. The increase in load toward the end was extremely small, leading to the conjecture that the reached force (F) of 193 kN corresponds approximately to the reference ultimate load-carrying capacity. For Girder 2, an ultimate load-carrying capacity of 240 kN, corresponding to a relative increase of 24% compared to the reference girder, was measured. At that stage, the ultimate tensile capacity of the CFRP strips was reached.

Strain Analysis and Crack Distribution

At the moment of the test end for Girder 1, the ultimate concrete strain in compression (ε_c) at midspan was 0.23%. With a

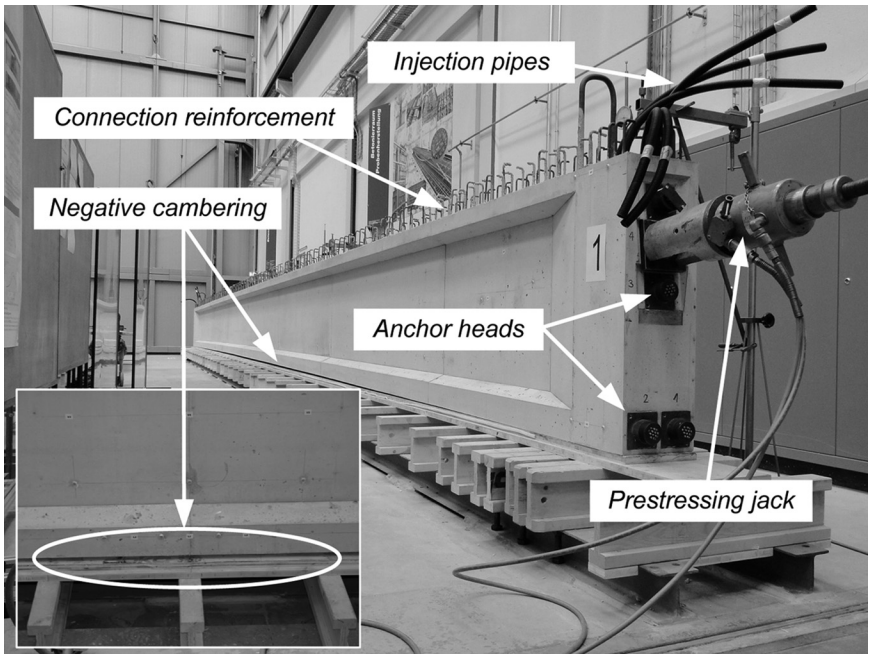

Fig. 4. Prestressing of the prestressed concrete girder(s) (images by Julien Michels)

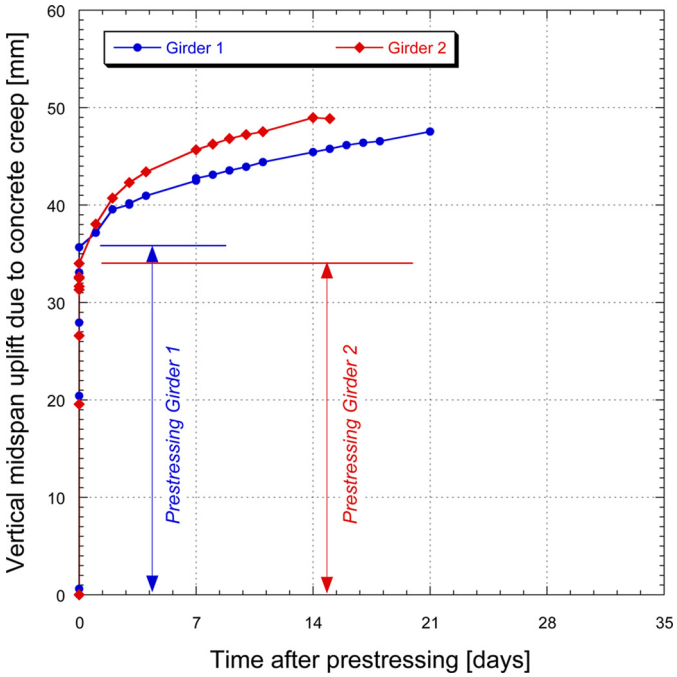

Fig. 5. Vertical midspan uplift due to prestressing and concrete creep over time

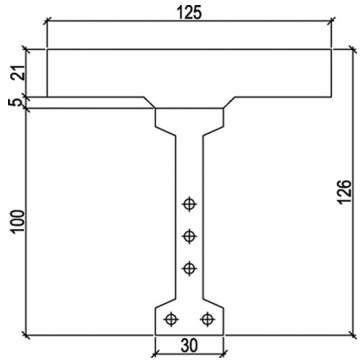

Fig. 6. Cross section of the casted girder (dimensions in centimeters)

sufficient stroke, concrete crushing could most likely be reached. For the strengthened Girder 2, the ultimate load-carrying capacity of 240 kN by tensile failure of the CFRP strips was reached at a concrete compressive strain level at midspan of approximately 0.15%. For both girders, all measured concrete strains plotted against the load F are shown in Fig. 14. The previously explained stiffer structural behavior of the strengthened girder is also visible in the strain behavior. It is important to notice that, for both the reference and the strengthened girders, the strain gauges used for capturing the compressive strains on top were mounted after the cable and CFRP strip prestressing. This indicates that the measured and presented values for ε_c in Fig. 14 also include a negative concrete strain in tension on the deck side prior to the static loading, and are hence not to be compared with the calculations. Evolution of the different CFRP tensile strains (ε_f) with growing load F is presented in Fig. 15(a). As mentioned, failure in Girder 2 was eventually obtained by tensile failure in the CFRP strip, measured with a maximal CFRP strain in tension ($\varepsilon_{f,u}$) of 1.58% shortly before failure. A photo of the CFRP strips after test end with the carbon filaments is shown in Fig. 15(b). The first flexural crack appeared in the central part in the region of the maximum moments; hence, strain gauges on the CFRP strips at locations x = 7,800, 8,990, and 9,000 mm indicate a first stiffness loss at the previously mentioned cracking load (F_{cr}) of 110 kN (Fig. 15). Afterward, flexural and shear cracks gradually moved toward the supports. Strain gauges CFRP10.1 and CFRP10.2, for instance, started deviating from the linear elastic region at a load slightly higher than 150 kN. Eventually, cracks reached the area located 3 m from the supports at a force level higher than 210 kN [Fig. 15(a)]. CFRP

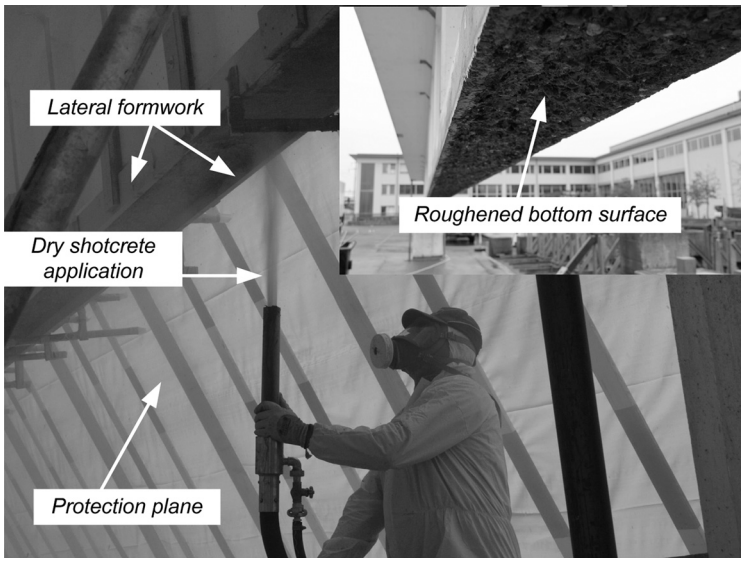

Fig. 7. Roughened bottom surface after waterjetting at high pressure and dry shotcrete application (images by Julien Michels)

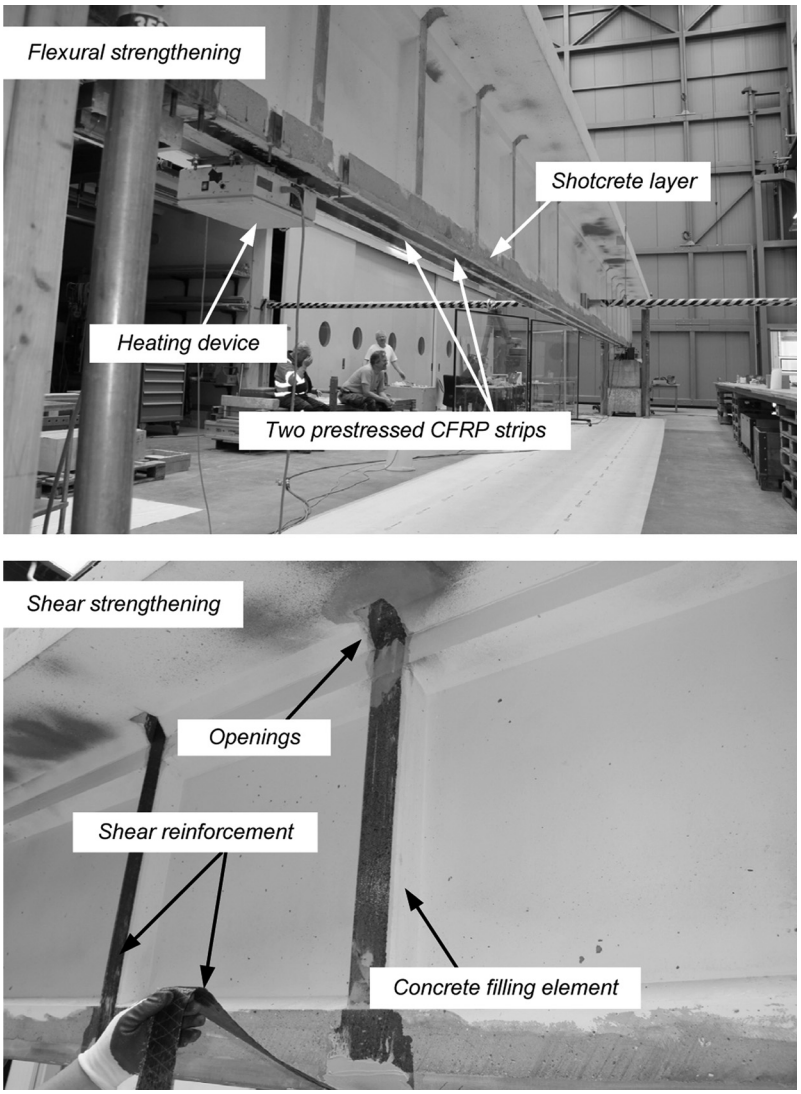

Fig. 8. Flexural and shear reinforcement for the large-scale girder (images by Julien Michels)

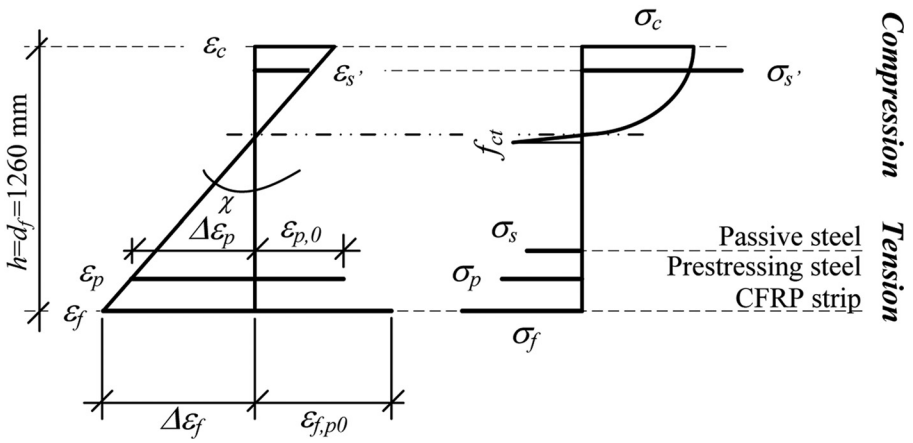

Fig. 9. CSA: indication of the strain state at the moment of CFRP prestressing and anchoring

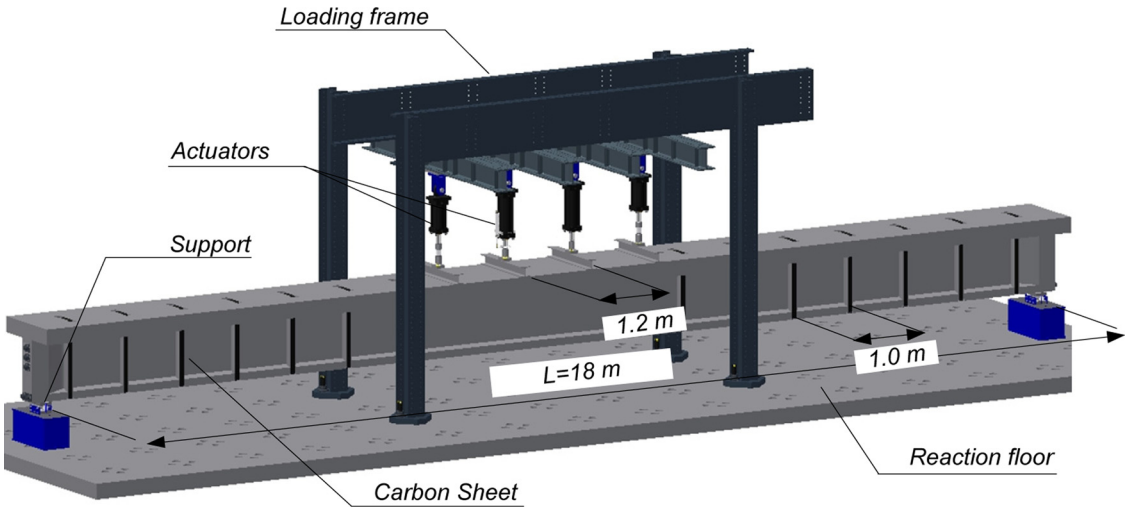

Fig. 10. Test setup for the large-scale static tests

tensile-strain evolution distributed over half the girder length is given in Fig. 16. From the initial prestrain ($\varepsilon_{fp,0}$), it was possible to obtain a total strain increase in tension ($\Delta\varepsilon_f$) of 1.0% at midspan.

Failure Mode

The most important information to be retained from the tests is the tensile failure of the CFRP strips. As mentioned in the introduction, the most inconvenient aspect of initially unstressed and externally bonded composite reinforcement in concrete retrofitting is mostly the fact that the materials' excellent mechanical performance in tension is rather badly exploited as a result of a premature strip debonding. Also, for prestressed strips, debonding is the most common failure mode. In this case, it was possible to fully use the tensile capacity, and hence to obtain the highest strengthening level possible. The static system with a large span of 18 m indicated that both anchorage zones were kept apart by approximately 15 m, possibly having the effect of avoiding a premature debonding, as was observed with short-span beams in Aram et al. 2008). Additionally, one strong contribution to the overall load-carrying capacity might have been the presence of the CFRP wraps for the shear strengthening. Because they were installed after application of the flexural strengthening, they are completely wrapped around the strip, and hence represent a barrier to a premature debonding. This observation is a strong argument in favor of such a shear reinforcement, even when not necessary from a design point of view for shear, because it might strongly improve the overall structural behavior in bending. A further reason for the CFRP tensile failure was the fact that the anchorage zone remained uncracked on the bottom side.

Structural Ductility

In the "Force Deflection" section, a strengthening efficiency of 24% was presented when comparing the ultimate load of the strengthened girder (240 kN) to the maximal force of the reference beam (193 kN). From a structural design point of view, it is also necessary to consider a few ductility aspects for Girder 2. Three ductility index calculations in terms of curvature, deflection at midspan, and energy dissipation are discussed and evaluated for the retrofitted structure.

Because both the upper concrete strain in compression as well as the CFRP strain in tension at midspan are available (measurements), it is possible to determine the curvature at several loading steps. By applying the rule of proportion (sections remain plane), a

curvature at a steel yielding (χ_y) of 3.131×10^{-6} (1/mm) can be obtained for the lowest cable positions at midspan. At failure, the corresponding curvature (χ_u) is equal to 9.178×10^{-6} (1/mm). The curvature ductility index (μ_χ) is equivalent to the ratio between curvature at both failure and yielding [Eq. (1)]

$$\mu\chi = \frac{\chi_u}{\chi_y} \tag{1}$$

where subscripts y and u = characteristic values at yielding and ultimate state, respectively. In this case, the index takes a value of 2.93 and thus is higher than the minimum value of 2.6 required by the International Federation for Structural Concrete (fib) Bulletin 14 (fib 2001) for concrete types higher than C35/45. At failure, an additional steel strain in the cables ($\Delta\varepsilon_p$) of 0.93% can be calculated. This value is higher than the requested 0.5% steel strain at failure for conventional reinforcement in a RC element strengthened with an unstressed EBR CFRP strip requested by the standard ACI440.2R-8 (ACI 2008). To summarize, retrofitted Girder 2 satisfies common design requirements. It is noteworthy that the observed additional tensile strain ($\Delta\varepsilon_f$) of 1.0% in the CFRP strips at failure is far higher than the ultimately tolerated value of 0.8% by, for instance, standard SIA166 (SIA 2004) given for initially unstressed strips.

The classic deformability index (μ_δ) relates the deflection at failure to the one at steel yielding (Eq. 2)

$$\mu_\delta = \frac{\delta_u}{\delta_y} \tag{2}$$

For Girder 2, the deformability index takes the value 2.1 (see Table 3). Even though the value is smaller than the one comparing the respective curvatures, a clear increase between the midspan displacement at yielding and the one at ultimate load is seen.

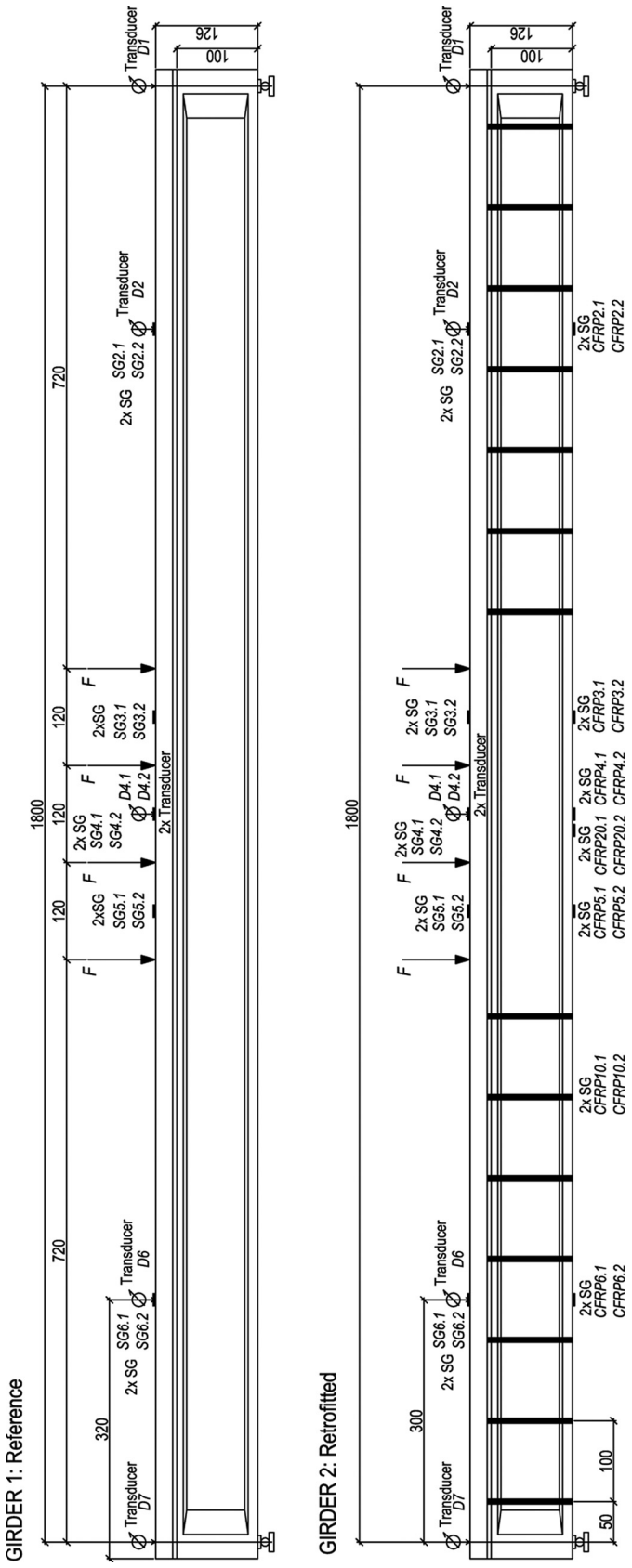

Fig. 11. Measurements configuration (dimensions in centimeters)

Table 3. Key Results of the Static Girder Tests

Parameter	Girder 1	Girder 2
δ_{cr} (mm)	22	23
F_{cr} (kN)	95	110
δ_y (mm)	100	100
F_y (kN)	160	190
δ_u (mm)	260	208
F_u (kN)	193	240
$\varepsilon_{c,\max}$ (%)	0.23	0.15
$\varepsilon_{f,\max}$ (%)	—	1.58
Failure mode	Toward concrete crushing	CFRP tensile failure

Numerical Parameter Study

Fig. 17 shows the force-deflection curves for the static loading test with the retrofitted girder compared to numerical simulations with the previously described CSA. Several prestrain levels ($\varepsilon_{fp,0}$), including 0.1, 0.2, 0.3, 0.4, 0.5, and eventually 0.58%, were calculated. The simulations for Fig. 17 were all carried out until tensile failure of the CFRP strip, assuming the same failure type for all prestrain levels as observed in the experimental test with an initial prestrain of 0.58%. Additionally, a limitation for the ultimate load-carrying capacity defined by a maximum additional strip strain in tension ($\Delta\varepsilon_{fp}$) of 0.8%, as given by SIA166 (SIA 2004), is indicated. It is important to note that the 0.8% represents an additional strain value to the initial prestrain value ($\varepsilon_{fp,0}$). In general, a good agreement between the experimental and numerical curves for an identical strip prestrain level of

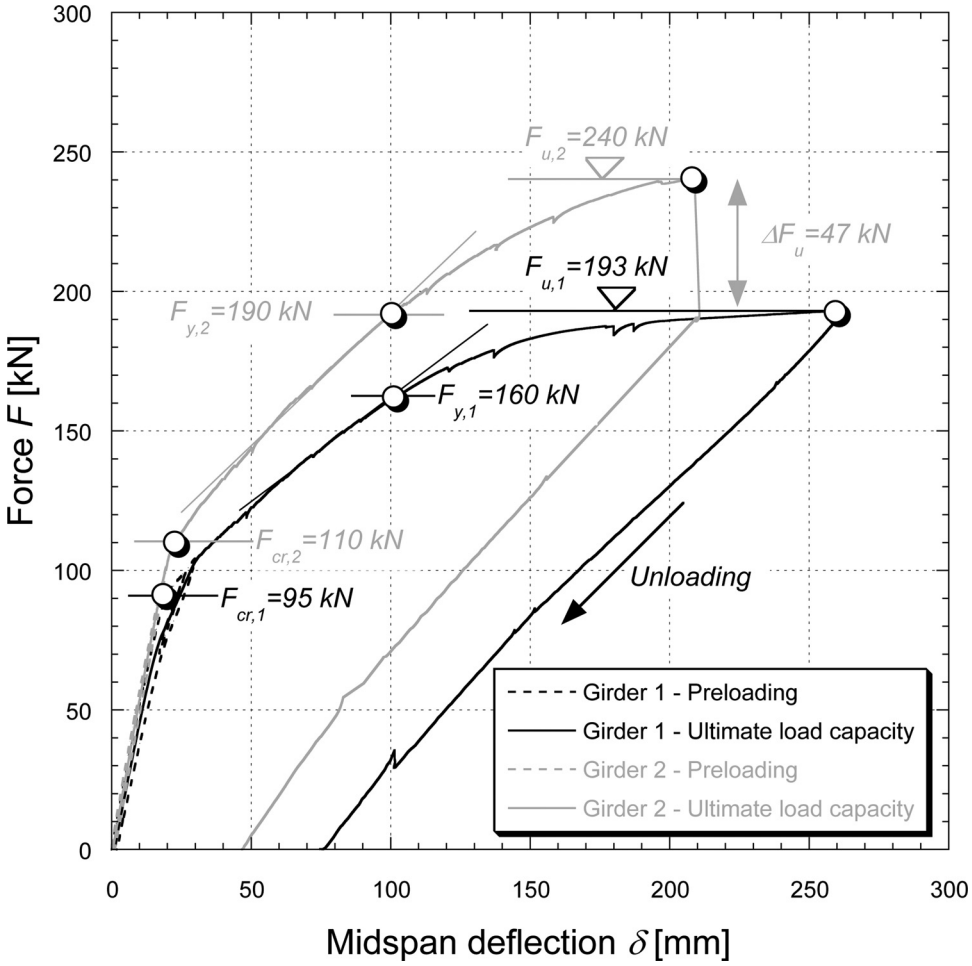

Fig. 12. Force-deflection (midspan) curves of Girders 1 and 2 up to the ultimate load-carrying capacity

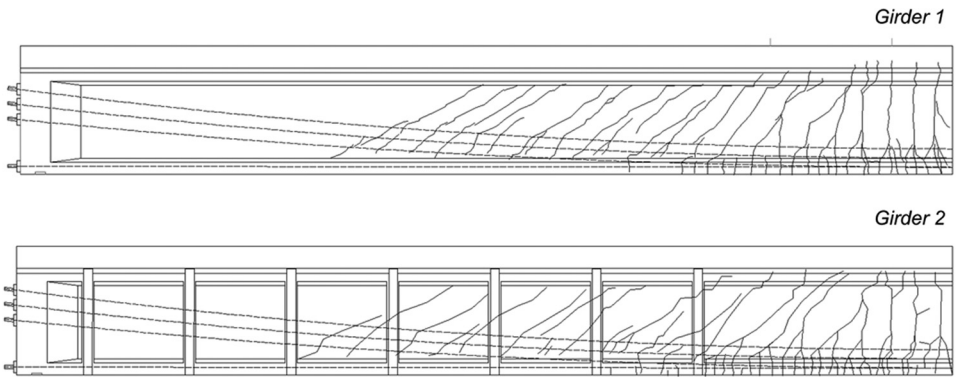

Fig. 13. Final crack pattern after test end (support to midspan)

0.58% corresponding to the static loading test is observed. The effect of a higher CFRP prestrain level on the cracking load is not extremely pronounced; the calculated values range between both experimental values for the reference and the retrofitted girder presented earlier in the paper (approximately 90–110 kN). However, regarding the yielding load, an increase with a higher initial prestress level is obvious. The corresponding deflection does not significantly change. Because, in the first case, tensile failure of the strip is assumed for all calculated scenarios, ultimate load is identical. A gain in structural stiffness after cracking goes together with a reduced ductility in terms of deflection at failure when a higher prestrain level is applied. In this case, the deformability index decreases with a growing CFRP prestrain. These observations are in agreement with classic prestressed concrete theory and technique. When simulating with the aforementioned 0.8% maximum strip strain as the debonding criterion, ultimate load-carrying

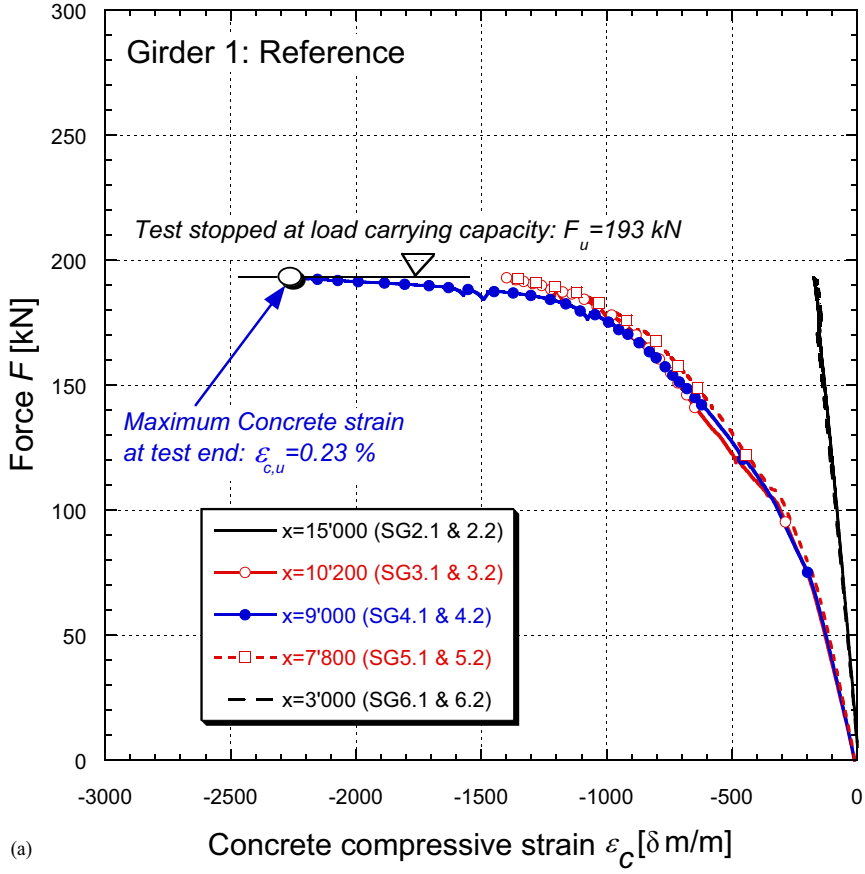

(a)

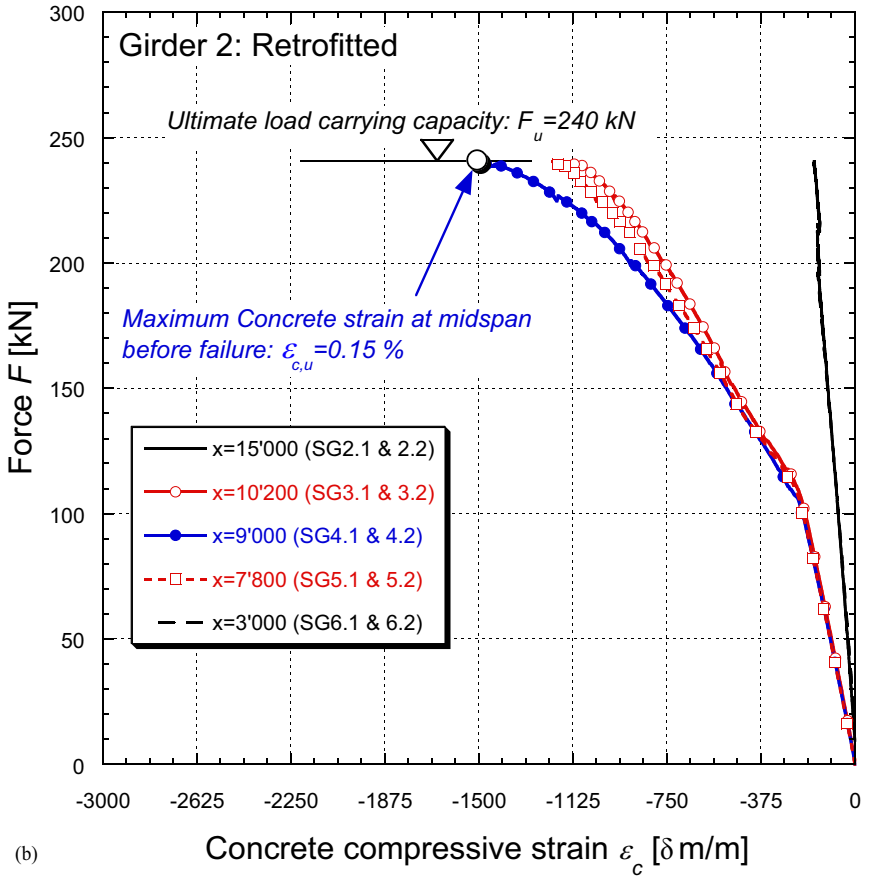

(b)

Fig. 14. Force-compressive concrete strain at midspan for both Girders 1 and 2

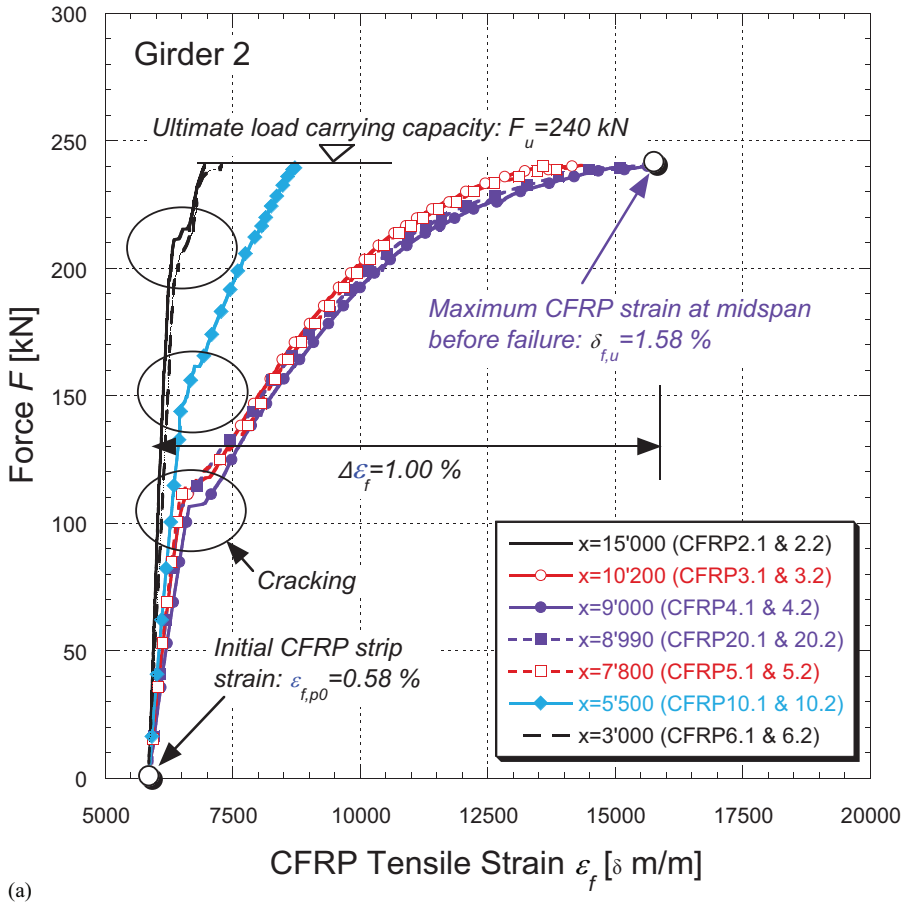

(a)

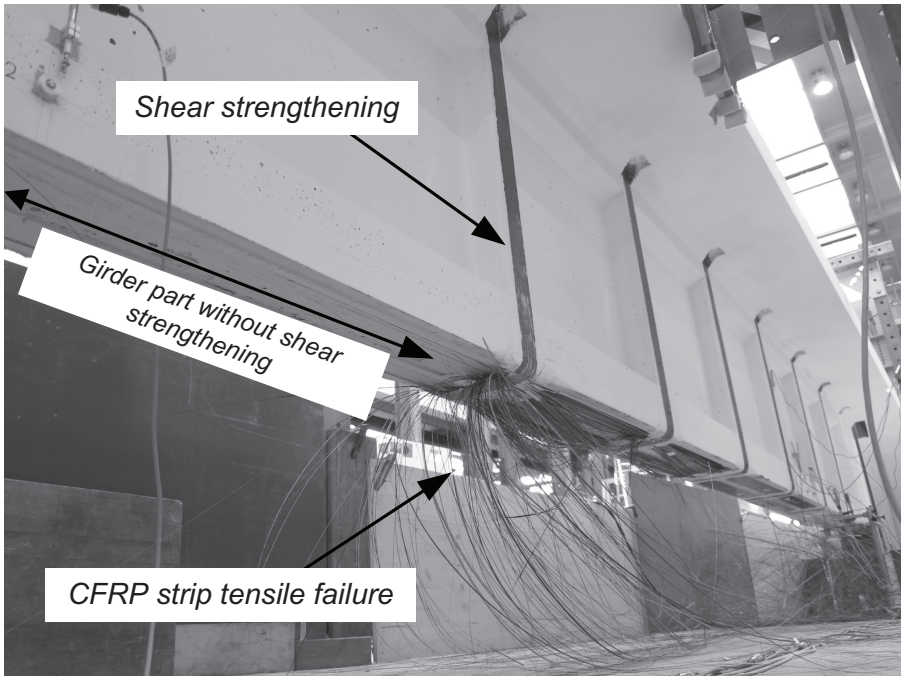

(b)

Fig. 15. Force-CFRP tensile strain (F, ε_f) diagram and photo of the CFRP strips after tensile failure (image by Julien Michels)

capacity is reached at the same deflection level, regardless of the initial strip prestrain. However, a higher value of the latter indicates a higher ultimate bearing capacity. Steel yielding is reached in all of the simulated cases. Eventually, contrary to the CFRP tensile failure criterion, the previously discussed deformability index (μ_δ) is not affected when the 0.8% criterion is used.

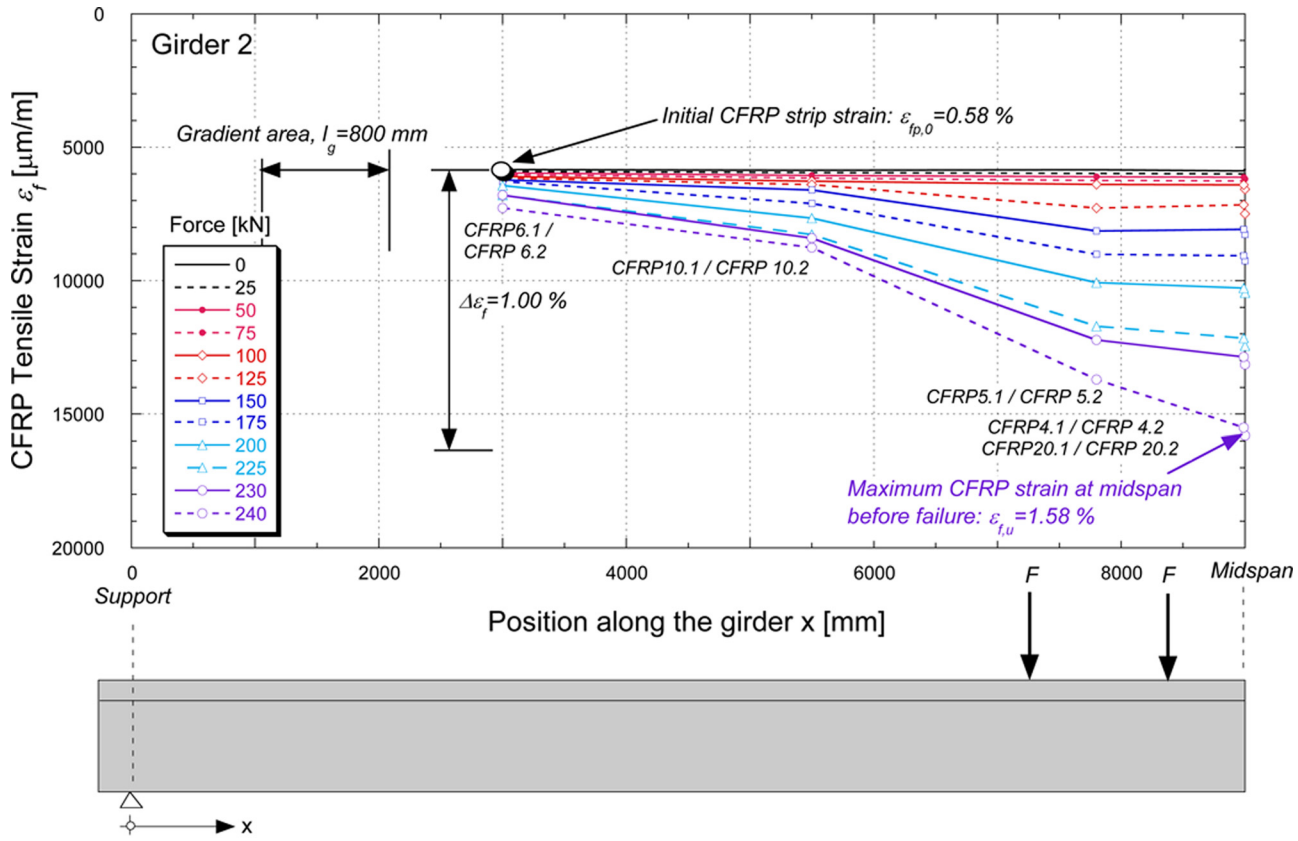

Fig. 16. CFRP tensile strain [ε_f; including the prestrain ($\varepsilon_{fp,0}$) = 0.58%] evolution over the horizontal girder axis with growing load (in kilonewtons) (axis not to scale)

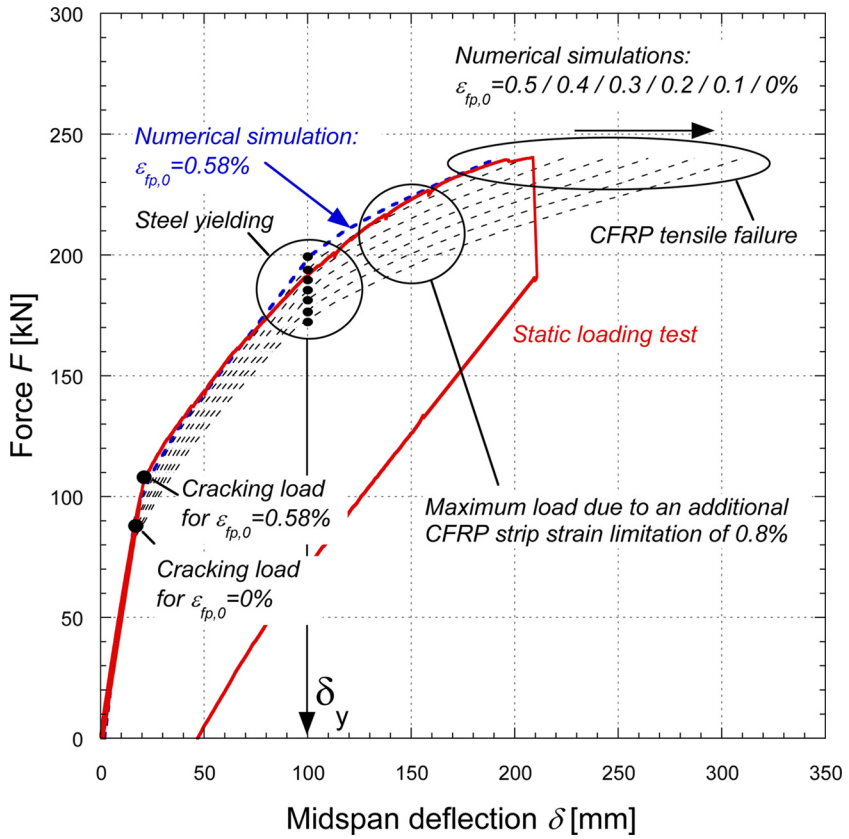

Fig. 17. Numerical simulations with various prestrain levels ($\varepsilon_{fp,0}$)

Conclusions

This paper presents an application of a strengthening method together with an experimental demonstration of its structural efficiency. Several conclusions can be drawn from the results:

- For practical applications, dry shotcrete seems to be a feasible solution for leveling an initially cambered beam or girder in case an additional CFRP strip reinforcement has to be installed. The application requires qualified operators, but exhibits good results in terms of bond to the concrete substrate. Even though certain preparation works (for instance, a lateral formwork prior to the shotcrete application) are necessary, the overall application time is fast.
- The feasibility of the application of the prestressed CFRP strips with gradient anchorage was proven in the present case. However, further investigation of the applicability on narrow girder geometries and dense reinforcement configuration in the bottom flange is necessary.
- For the present case, flexural strengthening by means of prestressed CFRP strips resulted in a clear enhancement of the cracking, yielding, and ultimate load compared to the unstrengthened girder of 16, 19, and 24%, respectively. Additionally, ductility of the structure up to failure was guaranteed.
- The ultimate load of the retrofitted structure was eventually reached by tensile failure of the CFRP strip. The fact that a CFRP strip debonding was avoided indicates a sufficient bond of the total CFRP/epoxy/shotcrete/concrete system as well as a good material exploitation of the strips in this case.
- The listed positive aspects of this strengthening and subsequent static testing activities lead to the conclusion that the suggested retrofitting technique by prestressed composite laminates might be a useful and efficient method to strengthen deficient structural concrete elements in the future.
- The key factor is the strengthening efficiency in terms of load-carrying capacity. Afterward, it has to be demonstrated that the retrofitted structure exhibits sufficient ductility, such as required by fib Bulletin 14 (fib 2001). The presented verification regarding the curvature ratio of the cross section at ultimate and steel yielding stage seems to be an adequate method, because it guarantees a distinct steel yielding prior to reaching the ultimate load-carrying capacity. This verification is recommended by the authors.

Acknowledgments

The presented research is part of the joined multidisciplinary research project TULCOEMPA between Łódź University of Technology and Empa. The financial support of the Polish-Swiss Research Programme for Project PSRP-124/2010 is highly appreciated. This project was supported by a grant from Switzerland through the Swiss Contribution to the enlarged European Union. S&P Clever Reinforcement Company, S&P Polska, and Granjet Granella AG are acknowledged for their support in the preparation of the concrete elements and material provision. Detailed product information on the composite reinforcements can be found in the respective data sheets (S&P Clever Reinforcement Company AG 2013a, b, c, d). The help of the laboratory staff of Empa for the testing activities and the image correlation measurements is appreciated.

References

ACI (American Concrete Institute). (2008). "Guide for the design and construction of externally bonded FRP systems for strengthening concrete structures." *ACI 440.2R-8*, Farmington Hills, MI.

Aram, M., Czaderski, C., and Motavalli, M. (2008). "Effects of gradually anchored prestressed CFRP strips bonded on prestressed concrete beams." *J. Compos. Constr.*, 10.1061/(ASCE)1090-0268(2008)12:1(25), 25–34.

Bae, S. W., and Belarbi, A. (2013). "Behavior of various anchorage systems used for shear strengthening of concrete structures with externally bonded FRP sheets." *J. Bridge Eng.*, 10.1061/(ASCE)BE.1943-5592.0000420, 837–847.

Bakis, C., et al. (2002). "Fiber-reinforced polymer composites for construction—State-of-the-art review." *J. Compos. Constr.*, 10.1061/(ASCE)1090-0268(2002)6:2(73), 73–87.

Berset, T., Schwegler, G., and Trausch, L. (2002). "Verstärkung einer Autobahnbrücke mit vorgespannten CFK-Lamellen." *tec21*, 128(22), 22–29 (in German).

Blaschko, M., and Zehetmaier, G. (2008). "Strengthening the Röslautal Bridge using innovative techniques, Germany." *Struct. Eng. Int.*, 18(4), 346–350.

Cerullo, D., Sennah, K., Azimi, H., Lam, C., Fam, A., and Tharmabala, B. (2013). "Experimental study on full-scale pretensioned bridge girder damaged by vehicle impact and repaired with fiber-reinforced polymer technology." *J. Compos. Constr.*, 10.1061/(ASCE)CC.1943-5614.0000383, 662–672.

Czaderski, C., Martinelli, E., Michels, J., and Motavalli, M. (2012). "Effect of curing conditions on strength development in an epoxy resin for structural strengthening." *Composites Part B Eng.*, 43(2), 398–410.

DAfStb (Deutscher Ausschuss für Stahlbeton). (2012). *Guideline: Strengthening of concrete members with adhesively bonded reinforcement—Part 1*. Berlin.

DIN (Deutsches Institut für Normung). (1997). "Plastics—Determination of tensile properties—Part 5: Test conditions for unidirectional fibre-reinforced plastics (German version)." *DIN-EN-ISO-527-5*, Berlin.

El-Hacha, R., Wight, R., and Green, M. (2001). "Prestressed fibre-reinforced polymer laminates for strengthening structures." *Prog. Struct. Mater. Eng.*, 3(2), 111–121.

El-Hacha, R., Wight, R., and Green, M. (2003). "Innovative system for prestressing fiber-reinforced polymer sheets." *ACI Struct. J.*, 100(3), 305–313.

fib (International Federation for Structural Concrete) (2001). "Externally bonded FRP reinforcement for RC structures." *fib Bulletin 14*, Lausanne, Switzerland.

Harmanci, Y. (2013). "Prestressed CFRP for structural retrofitting: Experimental and analytical investigation." M.Sc. thesis, ETH Zürich, Zürich, Switzerland.

Hognestad, E. (1951). "A study of combined bending and axial load in reinforced concrete members." *Bulletin 399*, Univ. of Illinois Engineering Experiment Station, Urbana, IL, 129.

Kasan, J., Harries, K., Miller, R., and Brinkman, R. (2014). "Repair of prestressed-concrete girders combining internal strand splicing and externally bonded CFRP techniques." *J. Bridge Eng.*, 10.1061/(ASCE)BE.1943-5592.0000475, 200–209.

Kim, Y., Green, M., and Fallis, G. (2008). "Repair of bridge girder damaged by impact loads with prestressed CFRP sheets." *J. Bridge Eng.*, 10.1061/(ASCE)1084-0702(2008)13:1(15), 15–23.

Kotynia, R., Walendziak, R., Stöcklin, I., and Meier, U. (2011). "RC slabs strengthened with prestressed and gradually anchored CFRP strips under monotonic and cyclic loading." *J. Compos. Constr.*, 10.1061/(ASCE)CC.1943-5614.0000081, 168–180.

Meier, U. (1995). "Strengthening of structures using carbon fibre/epoxy composites." *Constr. Build. Mater.*, 9(6), 341–351.

Meier, U., and Stöcklin, I. (2005). "A novel carbon fiber reinforced polymer (CFRP) system for post-strengthening." *Proc., Int. Conf. on Concrete Repair, Rehabilitation and Retrofitting*, CRC Press, Taylor & Francis, Boca Raton, FL.

Meier, U., Stöcklin, I., and Terrasi, G. (2001). "Civil engineers can make better use of the strength of fibrous materials." *Composites in construction*, Swets & Zeitlinger, Lisse, Switzerland.

Michels, J., Sena-Cruz, J., Czaderski, C., and Motavalli, M. (2013). "Structural strengthening with prestressed CFRP strips with gradient anchorage." *J. Compos. Constr.*, 10.1061/(ASCE)CC.1943-5614.0000372, 651–661.

Michels, J., Staśkiewicz, M., Czaderski, C., Lasek, K., Kotynia, R., and Motavalli, M. (2014). "Anchorage resistance of CFRP strips externally bonded to various cementitious substrates." *Composites Part B Eng.*, 63 50–60.

Park, R., and Paulay, T. (1975). "Reinforced concrete structures." *Bulletin 399*, John Wiley & Sons, New York, 129.

Pellegrino, C., and Modena, C. (2009). "Flexural strengthening of real-scale RC and PRC beams with end-anchored pretensioned FRP laminates." *ACI Struct. J.*, 106(3), 319–328.

Petrou, M., Parler, D., Harries, K., and Rizos, D. (2008). "Strengthening of reinforced concrete bridge deck using carbon fiber-reinforced polymer composite materials." *J. Bridge Eng.*, 10.1061/(ASCE)1084-0702(2008)13:5(455), 455–467.

Polish Committee for Standardization. (1986). "Bridges—Loads." *PN-85/S-10030*, Warsaw, Poland.

Polish Committee for Standardization. (1991). "Bridges—Concrete structures, reinforced and prestressed—Design." *PN-91/S-10042*, Warsaw, Poland.

Puurula, A., et al. (2014). "Assessment of the strengthening of an RC railway bridge with CFRP utilizing a full-scale failure test and finite-element analysis." *J. Struct. Eng.*, 10.1061/(ASCE)ST.1943-541X.0001116, D4014008.

SIA (Schweizer Ingenieur- und Architektenverein). (2004). "Klebebewehrungen (externally bonded reinforcement)." *SIA166*, Zurich, Switzerland.

S&P Clever Reinforcement Company AG. (2013a). "S&P C-sheet 240: Technical data sheet." ⟨http://www.sp-reinforcement.eu/en/products/frp-strengthening-systems/technical-data-sheets/⟩.

S&P Clever Reinforcement Company AG. (2013b). "S&P 50/55 epoxy adhesive: Technical data sheet." ⟨http://www.sp-reinforcement.eu/en/products/frp-strengthening-systems/technical-data-sheets/⟩.

S&P Clever Reinforcement Company AG. (2013c). "S&P laminates CFK: Technical data sheet." ⟨http://www.sp-reinforcement.eu/en/products/frp-strengthening-systems/technical-data-sheets/⟩.

S&P Clever Reinforcement Company AG. (2013d). "S&P resin 220 epoxy adhesive: Technical data sheet." ⟨http://www.sp-reinforcement.eu/en/products/frp-strengthening-systems/technical-data-sheets/⟩.

Suter, R., and Jungo, D. (2001). "Vorgespannte CFK-Lamellen zur Verstärkung von Bauwerken." *Beton-Stahlbetonbau*, 96(5), 350–358 (in German) .

Wight, R., Green, M., and Erki, M. A. (2001). "Prestressed FRP sheets for poststrengthening reinforced concrete beams." *J. Compos. Constr.*, 10.1061/(ASCE)1090-0268(2001)5:4(214), 214–220.

Xue, W., Zeng, L., and Tan, Y. (2008). "Experimental studies on bond behaviour of high strength CFRP plates." *Composites Part B Eng.*, 39(4), 592–603.